

# Vibration of mitred and smooth pipe bends and their components

D. Redekop<sup>†</sup> and D. Chang<sup>‡</sup>

*Department of Mechanical Engineering, University of Ottawa, Canada K1N 6N5*

*(Received April 20, 2009, Accepted October 8, 2009)*

**Abstract.** In this work, the linear vibration characteristics of 90° pipe bends and their cylindrical and toroidal shell components are studied. The finite element method, based on shear-deformation shell elements, is used to carry out a vibration analysis of metallic multiple 90° mitred pipe bends. Single, double, and triple mitred bends are considered, as well as a smooth bend. Sample natural frequencies and mode shapes are given. To validate the procedure, comparison of the natural frequencies is made with existing results for cylindrical and toroidal shells. The influence of the multiplicity of the bend, the boundary conditions, and the various geometric parameters on the natural frequency is described. The differential quadrature method, based on classical shell theory, is used to study the vibration of components of these bends. Regression formulas are derived for cylindrical shells (straight pipes) with one or two oblique edges, and for sectorial toroidal shells (curved pipes, pipe elbows). Two types of support are considered for each case. The results given provide information about the vibration characteristics of pipe bends over a wide range of the geometric parameters.

**Keywords:** finite element method; pipe bend; natural frequencies; mode shapes.

---

## 1. Introduction

Pipe bends form essential components of all piping networks. The bends provide flexibility to the systems, and being connected to other components are subject to structural vibrations. Smooth pipe bends offer better flow characteristics, and more gradual variations in stresses. Mitred bends, comprising of oblique cylindrical shells welded together, may have less favorable flow and stress characteristics, but can offer economic advantages in some parametric ranges. Interest in the components stems from the fact that reinforcement provided for piping systems may provide sufficient rigidity so that the motion of the individual components may be considered independently.

A compilation of studies performed on mitred bends has recently been presented (Wood 2008). Extensive research has already been completed, dealing largely with stress and collapse analysis of single mitred bends. Aside from several recent studies (Chang and Redekop 2007, 2008), little attention has been paid to the study of the changes in behavior that occur as the multiplicity of the mitred bend is increased. As well, aside from a few studies (Baylac and Copin 1975, Redekop and Chang 2008), little work has been done on the topic of vibration of mitred bends. The significance

---

<sup>†</sup> Professor Emeritus, Corresponding author, E-mail: [dredkop@uottawa.ca](mailto:dredkop@uottawa.ca)

<sup>‡</sup> Research Associate, E-mail: [dchang@uottawa.ca](mailto:dchang@uottawa.ca)

of vibration characteristics of pipelines in their operation has been outlined, for example, by Wachel *et al.* (1990).

There is an immense literature dealing with the vibration of cylindrical shells. Studies on the vibration of complete cylindrical shells have been summarized in three major monographs (Leissa 1973, Soedel 2006, Blevins 1979). Some analytical work has been done on the vibration of oblique cylindrical shells (Hu and Redekop 2003), and on a cylindrical shell-torus assembly (Redekop 2004). Studies on the vibration of piping bends with a smooth curved pipe have been conducted by Salley and Pan (2002), Ming *et al.* (2002), and Orynyak *et al.* (2007). Recently, a study has been conducted on the vibrations of a curved pipe based on elbow finite elements (Carneiro *et al.* 2005). Experimental and numerical results were given in this latter study, and these were compared with results for a straight pipe of similar radius, thickness and center-line length.

In the first part of this study, the finite element method (FEM), based on shear-deformation shell elements, is used to study the linear vibration characteristics of metallic multiple mitred bends. Reference is also made to smooth bends. Both natural frequencies and mode shapes are determined. To validate the procedure, a comparison of natural frequencies is made with existing results for cylindrical shells (straight pipes) and sectorial toroidal shells (curved pipes, pipe elbows). The influence on the natural frequencies of the boundary conditions, of three geometric parameters, and of the multiplicity of the bend is determined. In the second part of the study the differential quadrature method (DQM) is used to determine the fundamental frequencies of oblique cylindrical shells, and of curved pipes. These geometries represent the constituent components of mitred and smooth pipe bends. Two types of boundary conditions are considered for each type of component. Based on the frequency data generated, regression formulas are derived which permit the prediction of the fundamental frequency of each component over a wide range of geometric parameters.

## 2. Geometry and material model

A schematic view of the pipe bend assemblies considered in the study is given in Fig. 1. All bends are  $90^\circ$ , and have the same tangent pipe structure. The 1M bend has a single fold with an oblique edge that makes an angle of  $\beta = 45^\circ$  with the normal to the tangent pipe axes. The 2M bend has two folds ( $\beta = 22.5^\circ$ ), and the 3M bend has three folds ( $\beta = 15^\circ$ ). The C bend has a smooth circular transition between the two tangent pipes. Details of the geometry for the 2M bend are given in Fig. 2. The main geometric characteristics are the nominal bend radius  $R$ , the mean cross-sectional radius  $r$ , the wall thickness  $h$ , and the lengths of the tangent pipes  $L_1$  and  $L_2$ . For the 1M model an artificial bend radius  $R$  is assigned, to ensure a tangent pipe structure identical to the other bends. For all models studied in this work, the two tangent pipes were taken as equal in length (i.e.,

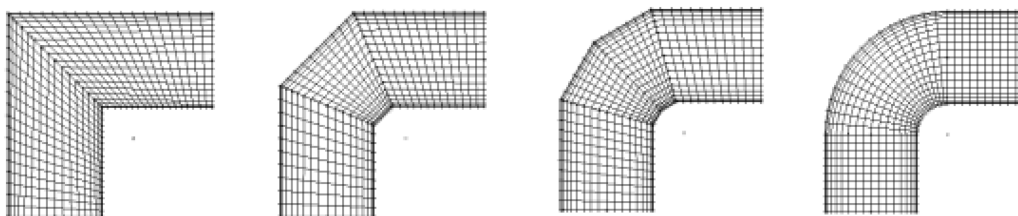


Fig. 1 Four configurations of  $90^\circ$  pipe bends - left to right; 1M, 2M, 3M and C

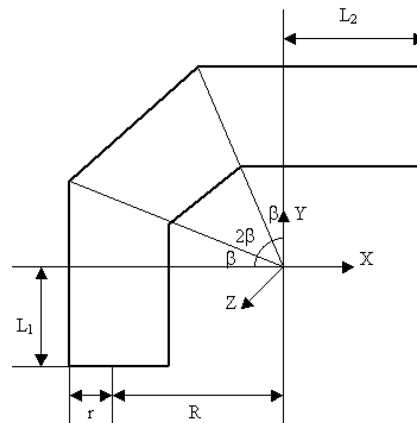


Fig. 2 Details of the geometry for the 2M mitred configuration

$L_1 = L_2 = L$ ), and were assumed integrally connected to the adjacent component. Stiffening rings, flanges, weld protrusions, and imperfections are not directly considered in the model. A free vibration analysis is conducted, i.e., there is no consideration of loadings on the surface or at the ends of the pipe structures.

In the current analysis of the mitred bends, the assemblies were assumed either clamped or free at the lower end of the vertical tangent pipe, and at the right end of the horizontal pipe. The boundary conditions at a clamped end were enforced by requiring all displacement and rotations on the boundary nodes to be zero. Symmetry in the geometry is present about a central vertical plane, as well as about the normal plane passing through the center of the bend, suggesting the possible use of half or quarter models in the analyses. However, to obtain all possible modes of vibration, including unsymmetrical ones, the analysis was for the full models in all cases.

When ring supports provide sufficient stiffness, the motion of the constitutive components becomes of interest. For mitred bends, the constitutive component is a cylindrical shell, with one or both ends oblique. For smooth bends, the constitutive component is a partial toroidal shell, and of lesser interest, a right-ended cylindrical shell.

The material for all models was taken as linear, isotropic, and elastic. The three material properties affecting the vibration behavior are the Young's modulus  $E$ , the Poisson's ratio  $\nu$ , and the mass density  $\rho$ . As results throughout the study are given for specific geometric cases, non-dimensionalization was not carried out, and all frequencies  $\omega$  are cited in Hz.

### 3. Linear finite element vibration analysis

The structural FEM program ADINA (ADINA 2003) was used to carry out the main analysis for the pipe bends, but the ANSYS code (ANSYS 2005) was also used in the validation. The shell element used in ADINA was the 16-noded isoparametric element, while that in ANSYS the 8-noded isoparametric element. These elements are both shear-deformation elements, belonging to the Reissner-Mindlin family (Hinton *et al.* 2003). For parts of the validation study, a 4-node flat shell element was also used in ADINA. The 16-noded isoparametric element is an intrinsic part of the ADINA software, and is shown herein to give results closely agreeing with those from the more

common low order elements. Results stemming from the NASTRAN program, mentioned in the validation, were based on a 4-node element.

For models with all edges free, such as considered in this study, rigid body modes exist. While the structural matrix is singular for such models, the software has provision to analyze these cases. For the solution of the eigenvalue problem several options were available in ADINA, of which the Lanczos method proved the most effective (Grimes *et al.* 1994).

The software used in the present study allows for a specification of element length ratio in a graded mesh, and a value of two was used in one validation case. This selection gave an element length at the support position two times that at the junction position. Grading of the mesh is known to be highly significant for stress concentration problems. For the current vibration problem, it was found that grading the elements in the axial direction did not greatly influence the results for the fundamental frequency.

#### 4. Validation and convergence for FEM study

While no vibration results for mitred bends were available in the literature to validate the FEM procedure, results were available for straight and curved pipes, and for an obliquely-cut cylindrical shell. The comparison of results, and an indication of the convergence of the FEM for those geometries, is presented in Tables 1, 2.

A comparison is first made for the vibration of straight and curved pipes. In two recent studies natural frequencies were given for both of these two geometries. The work of Carneiro *et al.* (2005) concerned a clamped-clamped (C-C) straight pipe, and a clamped-free (C-F) 90° curved pipe. Two finite element analyses were given, as well as an experimental one. The first finite analysis was

Table 1 Validation of FEM for natural frequency  $\omega$  (Hz) for straight and curved pipes

Mode	Carneiro <i>et al.</i> (2005) models				Redekop (2004) models			
	(a) Straight pipe: C-C				(a) Straight pipe: C-F			
	ALGOR	Expt.	ADINA 20×20	ANSYS 20×20	NASTRAN 64×20	DQM 28×27	ADINA 30×20	ANSYS 30×20
1	1320	1240	1246.1	1247.0	1578.3	1600.5	1617.9	1598.5
2	1640	1410	1617.1	1625.2	2016.9	2085.3	2154.4	2085.7
3	2340	2440	2173.4	2185.6	2795.7	2799.3	2806.9	2798.6
4	3880	2610	2426.2	2421.2	3524.0	3626.6	3870.3	3628.9
5	-	-	2665.8	2676.3	4394.4	4365.0	4499.1	4355.3
	(b) Curved pipe: C-F				(b) Curved pipe: C-C			
	ALGOR	Expt.	ADINA 20×20	ANSYS 20×20	NASTRAN 64×20	DQM 28×27	ADINA 40×30	ANSYS 40×30
1	440	370	448.1	467.4	2271.8	2273.1	2283.7	2271.6
2	830	620	491.2	471.2	2627.8	2628.3	2700.8	2623.5
3	1630	1040	860.3	863.7	2913.3	2920.6	3024.6	2909.1
4	1640	1640	876.0	880.7	3178.8	3198.8	3209.7	3181.9
5	1990	1670	1657.0	1635.6	3422.8	3441.3	3475.7	3427.1

Table 2 Convergence and validation of natural frequency  $\omega$  (Hz) for an oblique cylindrical shell - comparison with DQM results of Hu and Redekop (2003) for C-C geometry

Mode	DQM	FEM - untapered mesh			2:1 taper
	22×44	12×24 -16N	24×48 - 16N	48×94 - 4N	24×48 - 16N
1	806.3	824.6	825.2	835.3	825.1
2	-	835.3	835.7	849.9	835.6
3	959.4	957.8	958.1	968.0	958.1
4	-	958.2	958.7	970.0	958.6
5	1034.5	989.1	990.0	1006.5	990.0
6	1040.7	1003.5	1003.7	1017.3	1003.7
7	1227.4	1217.6	1218.8	1249.2	1218.8
8	1231.7	1217.9	1218.9	1315.0	1218.9
9	1331.3	1308.1	1307.8	1327.0	1307.8
10	1336.3	1321.1	1320.8	1404.6	1320.8

based on a newly developed semi-analytical curved pipe finite element, while the second one made use of the commercial ALGOR program. In the experimental work the natural frequencies were found with the aid of an electromagnetic shaker and a piezoelectric accelerometer. It was found that the two sets of finite element results agreed fairly closely, but were generally higher than the experimental results.

The work of Redekop (2004) concerns again straight and curved pipes, but the boundary conditions are now C-F for the straight pipe, and C-C for the curved pipe. An FEM solution is given, as well as one based on the DQM. The FEM makes use of the commercial NASTRAN program, in which a 4-noded flat shell element is available. The DQM analysis makes use of a procedure introduced by Bert and Malik (1996) in a study on cylindrical shells. In the work by Redekop (2004) the governing equations are those of the Sanders-Budiansky linear shell theory (Budiansky 1968). This shell theory does not account for shear effects, but is recognized as one of the most accurate of the first-order theories. It was found that the FEM and DQM results showed excellent agreement for both of the pipe geometries considered.

A comparison of the results of Carneiro *et al.* (2005) and of Redekop (2004) with the current results is given in Table 1. A 16-node element was used for ADINA and an 8-node element for ANSYS. The mesh sizes varied, as indicated in the table. In the mesh sizes quoted for the current FEM and DQM approaches the first and second integers indicate, respectively, the elements or sampling points in the axial and circumferential direction. The material properties for the Carneiro *et al.* (2005) models were  $E=200$  GPa,  $\nu=0.3$ , and  $\rho=7850$  kg/m<sup>3</sup>. For the Redekop (2004) models, the properties were  $E=207$  GPa,  $\nu=0.3$ , and  $\rho=7800$  kg/m<sup>3</sup>.

The straight pipe model of Carneiro *et al.* (2005) had a cross-sectional radius of  $r=0.05$  m, a length of  $L=0.382$  m, and a thickness of  $h=2$  mm, while the curved pipe had a cross-sectional radius of  $r=0.05$  m, a pipe bend radius of  $R=0.2$  m, and a thickness of  $h=2$  mm. The comparison values quoted herein were scaled from Fig. 5 of Carneiro *et al.* (2005) or taken from those quoted by Orynyak *et al.* (2007). The current FEM results found using ADINA and ANSYS show excellent agreement with each other for all the five cited frequencies. The fundamental frequency found in the current FEM analysis also agrees well with the experimental fundamental frequency for the straight pipe, and with the ALGOR fundamental frequency for the curved pipe. There are

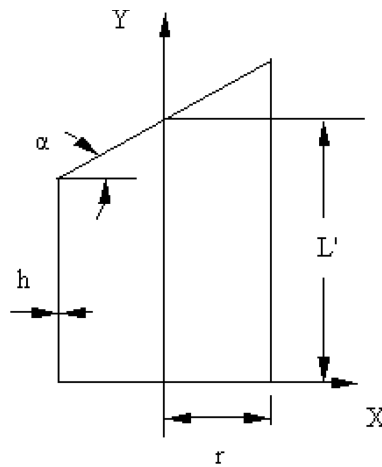


Fig. 3 Geometry of cylindrical shell (straight pipe) with single oblique edge

indications that some modes are absent in either the experimental or numerical results.

The straight pipe model of Redekop (2004) had  $r=0.0858$  m,  $L=0.176$  m, and  $h=7.11$  mm, while the curved pipe had  $r=0.0858$  m,  $R=0.2286$  m, and  $h=7.11$  mm. The current ADINA and ANSYS results again show excellent agreement with each other. There is also good agreement with the previous NASTRAN and DQM results, for both the straight and curved pipes, with differences in the fundamental frequency being less than 2.6%. For all the comparisons of Table 1, it is noted that the ADINA results contain a full complement of modes relative to those of the other approaches.

A comparison is next made for the natural frequencies of a cylindrical shell with an oblique edge (Fig. 3), geometrically resembling one half of a 1M mitred bend. In a study by Hu and Redekop (2003), a semi-analytical DQM solution was given for this problem. In the solution the surface of the shell was first developed onto a plane, and the resulting irregular domain then mapped, using blending functions, onto a square domain. The vibration analysis was carried out in the square domain using the transformed Sanders-Budiansky linear shell theory equations (Budiansky 1968). Results quoted by Hu and Redekop (2003) were for the fundamental frequency (in rad/s) only, but access to the DQM program was obtained, and for the current study the first ten frequencies were calculated, recorded in Hz.

A comparison of the results stemming from Hu and Redekop (2003) with the current ADINA results is given in Table 2. The cylindrical shell had a radius of  $r=0.1$  m, a mean axial length of  $L'=0.3$  m, and a thickness of  $h=1$  mm (Fig. 3). The angle of obliquity  $\alpha$  at the top end of the shell was  $30^\circ$ , and the material properties were  $E=183$  GPa,  $\nu=0.3$ , and  $\rho=7492$  kg/m<sup>3</sup>. For this case a fundamental frequency of 5066 rad/s (806.3 Hz) is quoted by Hu and Redekop (2003). The comparison with the current ADINA results in Table 2 includes a full set of results from the DQM, and four sets of results from the FEM. Three of the FEM results are for uniform meshes, and one is for a graded mesh, having element axial length at the perpendicular edge twice the axial length at the oblique edge. For the uniform (untapered) meshes both a 16 and a 4-node element are used. In the mesh sizes quoted, the first and second integers again indicate, respectively, the elements or sampling points in the axial and circumferential direction. Two frequencies are apparently absent from the DQM results, possibly arising from a difficulty in the software to determine some near-

equal or equal roots.

There is close agreement in the various results, with the difference in the fundamental frequency being less than 3.7%. The 4-node element gives slightly higher results than the 16-node element, but the agreement is very consistent up to the tenth mode. The results obtained from the tapered mesh using 16-node elements agree with the results of the uniform mesh to within 1%. It is clear that a 12×24 16-node mesh is sufficient for this geometry. While no comparison could be made with vibration results for mitred bends, it is clear that the current FEM approach gives reliable results for the components of mitred and smooth pipe bend geometries.

## 5. Results for mitred bends

FEM results from the ADINA program are presented in Tables 3, 4 and Figs. 6, 7 and 9, indicating the effect on the natural frequencies of changes in the boundary conditions, wall thickness, cross-sectional radius, length of tangent pipe, and type of bend configuration. The standard parametric model has a cross-sectional radius of  $r=0.15$  m, a pipe bend radius of  $R=0.25$  m, a tangent pipe length of  $L=0.25$  m, and a wall thickness of  $h=4.81$  mm. The  $R$  value is a bend radius which is uniquely defined for the configurations 2M, 3M and C (see Fig. 2). For the 1M configuration the  $R$  value is a theoretical radius, used to describe an analogous shell assembly with a single fold. The boundary conditions for the standard model were free-free (F-F), while the material properties were  $E=200$  GPa,  $\nu=0.3$ , and  $\rho=7850$  kg/m<sup>3</sup>. The F-F boundary conditions

Table 3 Variation of the natural frequency  $\omega$  (Hz) for the boundary conditions C-C, C-F, and F-F for the 1M and C configurations ( $r=0.15$  m,  $R=0.25$  m,  $L=0.25$  m,  $t=4.81$  mm)

Mode	1M configuration			C configuration		
	C-C	C-F	F-F	C-C	C-F	F-F
1	689.8	128.6	145.8	820.1	131.9	152.1
2	690.8	140.9	146.6	841.7	147.3	155.5
3	696.7	209.4	181.2	941.2	230.7	198.4
4	700.1	214.1	192.8	1134.7	235.3	213.0
5	757.5	404.9	284.7	1143.0	430.6	305.4
6	904.9	411.1	290.0	1166.8	430.6	339.9

Table 4 Variation of the natural frequency  $\omega$  (Hz) with the type of configuration for the F-F boundary condition ( $r=0.15$  m,  $R=0.25$  m,  $L=0.25$  m,  $t=4.81$  mm)

Mode	Configuration					
	Straight	1M	2M	3M	C	
1	139.1	145.8	155.8	154.3	152.1	
2	145.5	146.6	157.7	156.2	155.5	
3	393.0	181.2	197.7	200.5	198.4	
4	401.5	192.8	209.3	212.8	213.0	
5	552.6	284.7	310.8	311.0	305.4	
6	696.3	290.0	329.6	331.9	339.9	

were selected, as they are the most likely experimental form. The FEM model consisted typically of a  $36 \times 36$  mesh of 16-node elements. A parametric study was carried out typically for one or two of the four basic configurations of Fig. 1. For the various studies the natural frequency  $\omega$  is given in Hz for the first six modes of vibration.

In Table 3 are given the results indicating the effect on the natural frequencies of changes in the boundary conditions. Two geometric boundary configurations are covered; the 1M and the C, and three types of boundary conditions; C-C, C-F, and F-F. The various results indicate that the 1M configuration is more flexible than the C configuration. For both configurations there is a significant drop in the fundamental frequency going from the C-C to either a C-F or F-F condition. A similar trend is recorded in a work for a straight pipe (Leissa 1973, Fig. 2.83).

The fundamental mode shapes for the 1M and C configurations of Table 3 for the C-C, C-F, and F-F boundary conditions are given in Fig. 4. For the C-C and F-F cases the fundamental mode spans the full geometry for both configurations, while for the C-F geometry large amplitude is largely restricted to that half of the structure distant from the support. The first six mode shapes for the 1M configuration for C-C boundary conditions are shown in Fig. 5. For this boundary condition there is symmetry about a central plane passing through the junction. Furthermore, as the junction restricts displacement similar to a clamped support, there is an indication that the vibration in each half of the 1M configuration may closely resemble the vibration of an oblique cylindrical shell of similar dimensions. Analysis using the DQM program, however, led to a fundamental frequency of 857.9 Hz for the oblique cylindrical shell, compared to the FEM value of 689.8 Hz value for the 1M geometry.

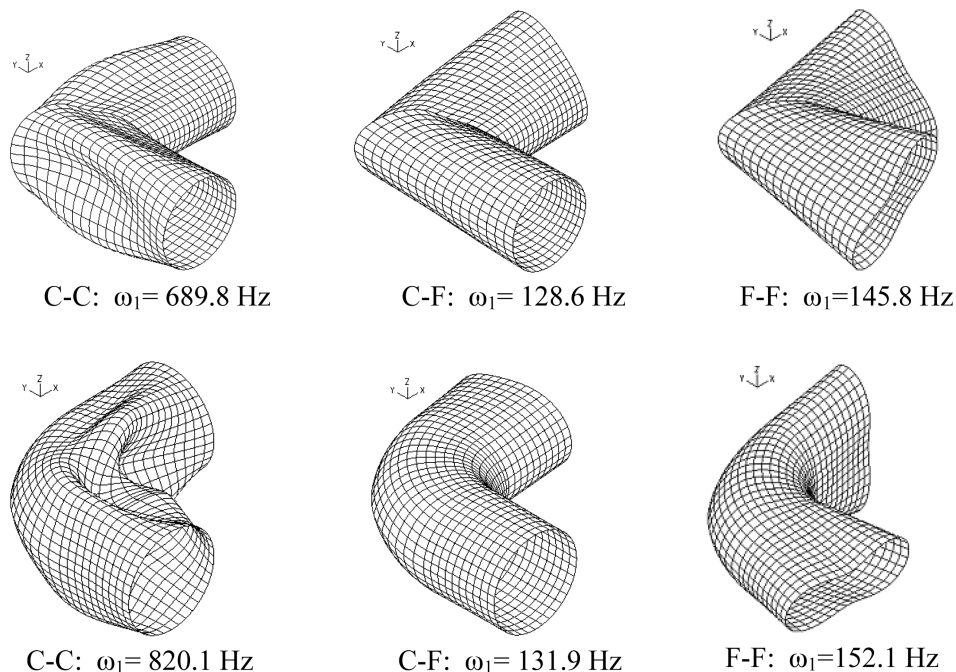


Fig. 4 Fundamental mode shapes for the 1M and C configurations for C-C, C-F, and F-F boundary conditions ( $r=0.15$  m,  $R=0.25$  m,  $L=0.25$  m,  $t=4.81$  mm). The FEM coordinate system does not follow the system of Fig. 2

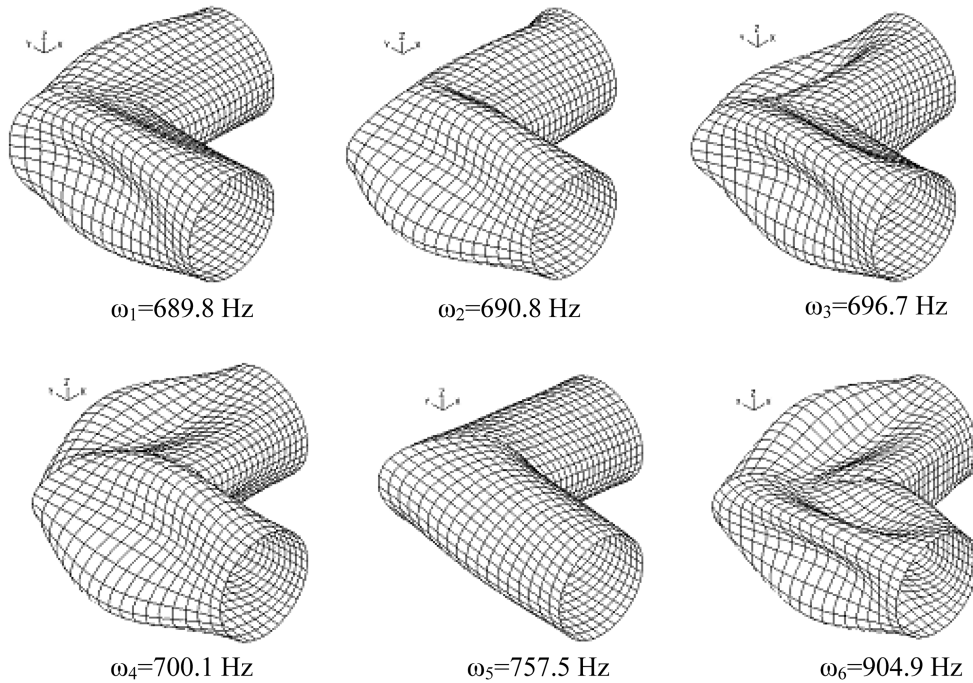


Fig. 5 First six mode shapes for the 1M configurations for C-C boundary conditions ( $r=0.15$  m,  $R=0.25$  m,  $L=0.25$  m,  $t=4.81$  mm)

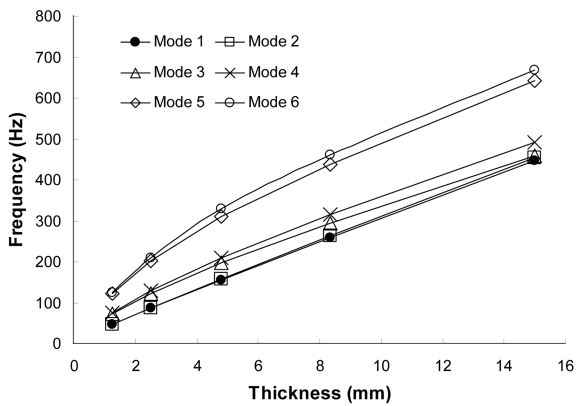


Fig. 6 Variation of the natural frequency  $\omega$  (Hz) with the wall thickness for the 2M configuration for the F-F boundary conditions ( $r=0.15$  m,  $R=0.25$  m,  $L=0.25$  m)

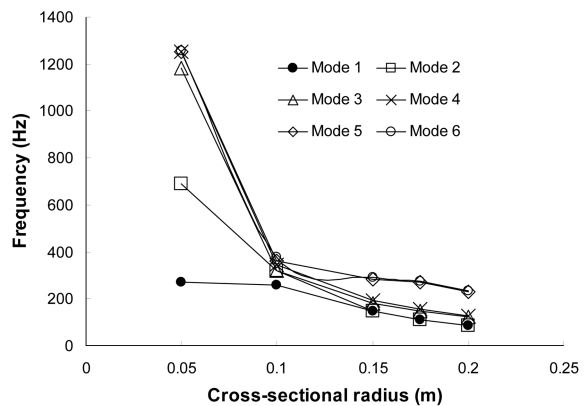


Fig. 7 Variation of the natural frequency  $\omega$  (Hz) with the cross-sectional radius for the 1M configuration for the F-F boundary conditions ( $R=0.25$  m,  $L=0.25$  m,  $t=4.81$  mm)

The effect on the natural frequencies of variation of the wall thickness for the 2M configuration is shown in Fig. 6. In this figure, and in Figs. 7-9, the results presented are for the F-F boundary conditions. With an increase in wall thickness there is a monotonic increase in the first six natural frequencies. For this geometry, a 12-fold increase in thickness leads to a 9.5-fold increase in the fundamental frequency.

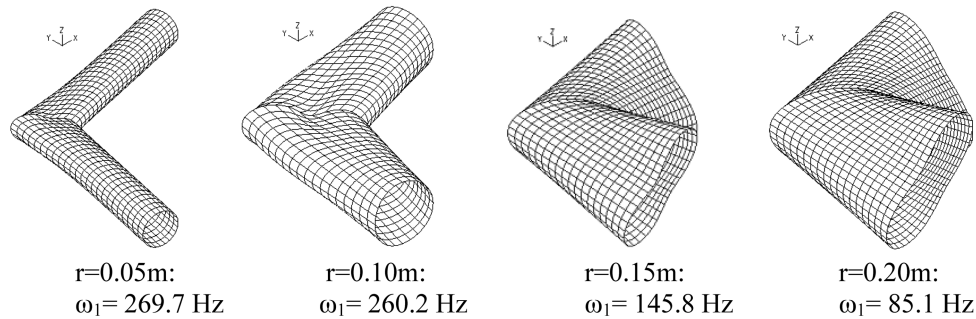


Fig. 8 Fundamental mode shapes for the 1M configuration for various cross-sectional radius values for F-F boundary conditions ( $R=0.25$  m,  $L=0.25$  m,  $t=4.81$  mm)

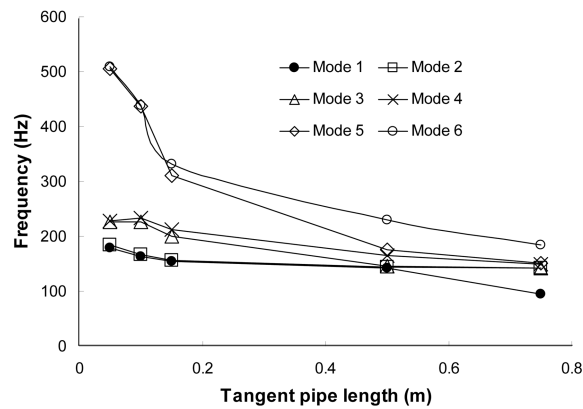


Fig. 9 Variation of the natural frequency  $\omega$  (Hz) with the length of the tangent pipe for the 3M configuration for the F-F boundary conditions ( $r=0.15$  m,  $R=0.25$  m,  $t=4.81$  mm)

In Fig. 7 are shown the results indicating the effect on the natural frequencies of the variation of the cross-sectional radius for the 1M configuration. With an increase in cross-sectional radius, there is a monotonic decrease in the fundamental frequency. For this geometry, a 4-fold increase in cross-sectional radius leads to a 3.2-fold decrease in the fundamental frequency. The fundamental mode shapes for the 1M configuration for four cross-sectional radius values for the F-F boundary conditions are given in Fig. 8. For the cases having the two lowest cross-sectional radii, large amplitude vibration is restricted to the junction area.

The results of Fig. 9 show the effect on the natural frequencies of the variation of the length of the tangent pipe for the 3M configuration. With an increase in the length of each tangent pipe there is a monotonic decrease in the fundamental frequency. For this geometry a 15-fold increase in the length of the tangent pipe leads to a 1.9-fold decrease in the fundamental frequency. A comparison considering the total axial length of the assembly is also of interest. The total axial length is taken as the arc length of the center line of the bend itself (approximately 0.4 m), plus twice the tangent pipe length. The longest case of Fig. 9 represents a 3.8-fold increase in total axial length relative to the shortest case, and a 1.9-fold decrease in the fundamental frequency.

For a straight cylindrical shell with F-F boundary conditions, a detailed coverage of the relationship between the fundamental frequency and the shell thickness, radius, and length is

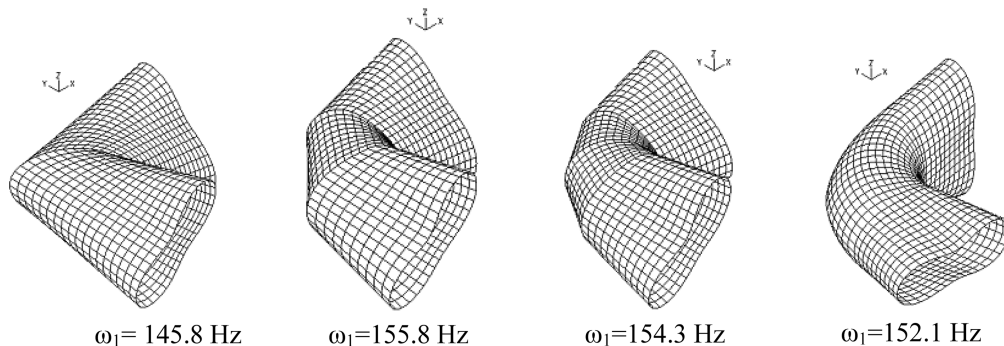


Fig. 10 Fundamental mode shapes for the 1M, 2M, 3M, and C configurations for F-F boundary conditions ( $r=0.15$  m,  $R=0.25$  m,  $L=0.25$  m,  $t=4.81$  mm)

available (Leissa 1973, Section 2.4.5). The Figs. 2.92-2.96 of his work give plots of the lowest frequency, for a given circumferential mode, versus ratios of the three geometric parameters. Similar trends in frequencies observed for the present shell assembly are observed for a straight pipe, namely an increase in frequency with an increase in thickness, and a decrease in frequency with an increase in radius or axial length. Earlier work has indicated that there is close agreement between theoretical and experimental frequencies for F-F boundary conditions (Leissa 1973, Fig. 2.97).

In Table 4 results are presented indicating the effect on the natural frequencies of the type of bend configuration. In this table natural frequencies are also given for a straight pipe having an axial length equal to the total center line length of the assembly of the C configuration. It is observed for the higher order bends, i.e., configurations 2M, 3M and C, that the natural frequencies are very similar in magnitude. The two lowest frequencies of the 1M configuration more closely resemble the frequencies of the straight pipe than those of the higher order bends.

The fundamental mode shapes for the 1M, 2M, 3M, and C configurations for the F-F boundary conditions are given in Fig. 10. Cross-sectional flattening at the two ends is observed, with the major cross-sectional axes lying roughly along perpendicular directions. For the 2M and 3M configurations, the amplitudes are relatively large only in the tangent pipe sections, as the weld lines provide a ring-like stiffening effect. Commencing from the 2M configuration, it is observed that when the number of segments is increased a trend in frequencies is established towards the curved pipe value, and when the number of segments is decreased a trend towards the straight pipe value.

## 6. Differential quadrature method

For the study of the vibration of the oblique cylindrical shell and curved pipe components, use was made of the DQM. A brief summary of this method is provided herein for completeness. The governing equations were those of the Sanders-Budiansky theory (Budiansky 1968), which is based on the Love-Kirchhoff assumptions. In the DQM, a grid of sampling points covering the domain must first be defined (Shu 2000). For both the oblique cylindrical shell and the curved pipe a two-dimensional grid of sampling points is required. The replacement of all derivatives in the governing equations with series of terms, that contain the product of a displacement function at a sampling point and a weighting coefficient, must next be made. Thus the  $r$ -th derivative of a generic function

of a single variable  $f(x)$  at the sampling point  $x_i$  is replaced by the series

$$\left. \frac{d^r f(x)}{dx^r} \right|_{x=i} = \sum A_{ik}^r f(x_h) \quad (1)$$

where the  $A_{ih}^r$  are the weighting coefficients of the  $r$ -th order derivative in the  $x$  direction for the  $i$ -th sampling point,  $f(x_h)$  is the value of  $f(x)$  at the sampling point position  $x_h$ , and the summation is over the number of sampling points in the  $x$  direction. This second step converts the problem from one of differential equations to one of linear algebraic equations.

In the DQM, the weighting coefficients are determined a-priori for the pre-selected grid, with the aid of selected trial functions. For the oblique cylindrical shell and for the curved pipe polynomial functions were used in the axial direction and trigonometric functions in the circumferential direction (Bert and Malik 1996). For the oblique cylindrical shell a preliminary step was required, namely the use of blending functions (Hu and Redekop 2003) to map the domain onto a rectangle. A regular spacing of the grid points was then introduced for the rectangle. For all DQM meshing schemes used, explicit formulas for the weighting coefficients  $A_{ih}^r$  are available (Shu 2000).

Use of the quadrature rule (1) for the derivatives in the governing equations leads to transformed algebraic DQM vibration equations. Enforcement of these equations at the grid points leads to the set

$$[K](U) = \lambda[M](U) \quad (2)$$

where the unknown ( $U$ ) contains the values of the displacement functions at the sampling points,  $\lambda$  is the unknown eigenvalue, and  $[K]$ ,  $[M]$  are the known 'stiffness' and 'mass' matrices.

For the DQM work of this study, programs developed earlier by Hu and Redekop (2003) for oblique cylindrical shells and by Redekop (2004) for straight and curved right-ended pipes were extended to enable the generation of results for the two individual components. In particular for the curved pipe, a program was developed to cover three types of boundary conditions, clamped, free and shear diaphragm. Extensive testing was conducted to ensure the accuracy of results for both programs.

## 7. Regression formulas for oblique cylindrical shells

Natural frequencies may be determined using the FEM or DQM in a lengthy numerical process. When quick approximations are desired, simple formulas may be used instead. The formulas are of two types, asymptotic formulas (derived directly from the theory) which are often valid only for a small range of limited interest, and regression formulas (derived from numerical work) which can cover a specified range of significant interest. In this section, regression formulas based on numerical DQM results are derived for the fundamental frequencies of cylindrical shells with one or two oblique edges. A cylindrical shell with one oblique edge approximates a tangent pipe in a mitred bend, whereas a cylindrical shell with two oblique edges approximates a central component of a 2M or 3M mitred bend (Fig. 1).

In consideration of earlier work (Leissa 1973), the fundamental frequency is assumed to have a direct relation with the square root of the quotient of the elastic modulus and mass density, and an inverse first power relation with the shell radius. Additionally, it is assumed that an exponential

variation of the frequency exists with the obliquity angle, the length ratio  $L'/r$ , and the thickness ratio  $r/h$ . The exponential indices for the latter three variations are determined by standard least squares regression analysis of DQM results. For both of the cylindrical shell edge cases two ranges of geometric parameters were specified

$$\begin{aligned} \text{Range 1: } & \alpha = 0 - \pi/4; L'/r = 1.5 - 4; r/h = 15 - 50 \\ \text{Range 2: } & \alpha = 0 - \pi/4; L'/r = 1.5 - 4; r/h = 50 - 200 \end{aligned} \tag{3}$$

The regression formula is assumed to have the form

$$\omega = b_o(E/\rho)^{0.5}(1/r)(\gamma)^{b_1}(L'/r)^{b_2}(r/h)^{b_3} \tag{4}$$

where  $\omega$  is the natural frequency in Hz,  $E$  is the elastic modulus in Pa,  $\rho$  is the mass density in kg/m<sup>3</sup>,  $\gamma = \pi/2 - \alpha$  is the complementary obliquity angle in radians,  $L'$ ,  $r$ ,  $h$  are length quantities given in m (see Fig. 3), and the  $b_i$  are regression coefficients. For the first of the two cylindrical shell edge cases (single oblique edge), the cylindrical shell was assumed to be clamped at the normal base, as well as at the oblique top. For the second of the two cases, the cylindrical shell was assumed to have two oblique edges, in a symmetrical arrangement. The boundary conditions at both oblique edges were considered clamped. Analysis was carried out on a half model, with  $L'$  representing the axial length from middle of the oblique edge to the central plane of symmetry.

The values of the coefficients of the regression formulas  $b_i$  for the two parametric ranges, for the two edge conditions, are given in Table 5. It is seen that the constants  $b_o$  in the formulas for the two edge conditions are roughly in the ratio of 2 to 1, as expected. For all four formulas derived, there is relatively low dependence of the frequency on the complementary angle of obliquity, strong dependence on the length ratio, and moderate dependence on the thickness ratio. Considering for a given edge condition the pairs of comparable exponential coefficients for the two ranges covered, small but significant distinctions are noted, as expected. Similar, but not identical dependence of the frequency on the three parameters should be present for the two ranges. For both of the edge components there is a significant increase in the importance of the  $b_1$  coefficient (length ratio) going from range 1 to range 2, indicating that for thinner shells the length ratio is more important than for thick shells.

A comparison of frequencies obtained from the regression formulas with previous values is given in Table 6 for right-ended and single-oblique-edged cylindrical shells. Cases 1-4 represent cylindrical shells having some geometric parameters lying outside of both of the parametric ranges defined, and close agreement is generally not seen. Cases 5-7 have all parameters within either of the two defined geometric ranges, and agreement within 5% is observed.

Table 5 Values of the coefficients in the DQM regression formulas for oblique cylindrical shells

Range	Edges	Geometry			Coefficients			
		$\gamma = \pi/2 - \alpha$	$L'/r$	$r/h$	$b_o$	$b_1$	$b_2$	$b_3$
1	1	$\pi/2 - \pi/4$	1.5-4	15-50	0.3177	0.2126	-0.8209	-0.4521
	2	$\pi/2 - \pi/4$	1.5-4	15-50	0.1653	0.1431	-0.9073	-0.4277
2	1	$\pi/2 - \pi/4$	1.5-4	50-200	0.3353	0.2937	-0.8075	-0.4701
	2	$\pi/2 - \pi/4$	1.5-4	50-200	0.1890	0.2468	-0.8652	-0.4752

Table 6 Comparison of the fundamental frequency  $\omega_1$  (Hz) from oblique cylindrical shell regression formulas with previous results for right-ended ( $\alpha=0^\circ$ ) and oblique cylindrical shells. Previous value for case 1 was found using FEM, cases 2-4 using series solution, cases 5-7 using DQM

Case	Reference	Boundary condition and geometry					Fundamental frequency		
		Edges	$\gamma_d$ ( $^\circ$ )	$r$ (m)	$L'/r$	$r/h$	Prev.	Regr.	% diff.
1	R&C 2008	1	90	0.05	7.64	25.0	1246	1579	-26.7
2	Leissa p93	1	90	0.0762	4.00	300	522	577	-10.5
3	Leissa p103	1	90	0.0489	8.13	19.2	1240	1730	-39.5
4	Leissa p101	1	90	0.2422	2.52	374	240	232	3.5
5	H&R 2003	1	90	0.1	2.00	100	1264	1241	1.8
6	H&R 2003	1	60	0.1	3.00	25.0	1560	1501	3.8
7	H&R 2003	2	60	0.1	3.00	100	420	409	2.5

## 8. Regression formulas for curved pipes

Regression formulas based on DQM results are derived in this section for the fundamental frequency of curved pipes having either clamped-clamped (CC) or shear-diaphragm shear-diaphragm (SD) boundary conditions. Similar to the case of the straight pipe, the fundamental frequency is assumed to have a direct relation with the square root of the quotient of elastic modulus and mass density, and an inverse first power relation with the shell radius. Additionally, it is assumed that an exponential variation of the frequency exists with the bend angle  $\psi$  (in radians), the bend to cross-section radius ratio  $R/r$ , and the thickness ratio  $r/h$ . The exponential indices for the latter three variations are again determined by a regression analysis of the DQM results. For both of the boundary conditions considered two ranges of parameters were specified

$$\begin{aligned} \text{Range 1: } \psi &= \pi/6 - \pi/2; R/r = 2.5 - 10; r/h = 15 - 50 \\ \text{Range 2: } \psi &= \pi/6 - \pi/2; R/r = 2.5 - 10; r/h = 50 - 200 \end{aligned} \quad (5)$$

The regression formula was assumed to have the form

$$\omega = b_o(E/\rho)^{0.5}(1/r)(\psi)^{b_1}(R/r)^{b_2}(r/h)^{b_3} \quad (6)$$

where  $\omega$  is the natural frequency in Hz,  $E$  is the elastic modulus in Pa,  $\rho$  is the mass density in  $\text{kg/m}^3$ ,  $\psi$  is the bend angle in radians,  $R$ ,  $r$ ,  $h$  are respectively the bend radius, cross-sectional radius, thickness in m, and the  $b_i$  are regression coefficients.

For the first of the two boundary conditions, the pipe was assumed to be clamped at both ends, forming a symmetrical arrangement. For the second of the boundary conditions, the curved pipe was assumed to have two edges with shear diaphragm supports, again in a symmetrical arrangement. For both cases the analysis was carried out on the full model.

The values of the coefficients  $b_i$  of the regression formulas for the two parametric ranges, for the two types of boundary conditions are given in Table 7. Contrary to expectation, it is seen that the constant  $b_o$  in the formula for the CC boundary condition is not higher than for the SD condition. It might be expected that the frequencies for the CC boundaries would be significantly higher than frequencies for the SD boundaries but this is not the case. There is a greater variation in the regression parameters for the curved pipe geometry than for the oblique cylindrical shell geometry. For the CC boundary condition there is a relatively low dependence on the bend angle, whereas for

Table 7 Values of coefficients in the DQM regression formulas for curved pipes

Range	Bdy.Cond.	Geometry			Coefficients			
		$\psi$	$R/r$	$r/h$	$b_0$	$b_1$	$b_2$	$b_3$
1	CC	$\pi/6-\pi/2$	2.5-10	15-50	0.2713	-0.6983	-1.0516	-0.2123
	SD				0.4729	-1.5474	-1.2690	-0.5893
2	CC	$\pi/6-\pi/2$	2.5-10	50-200	0.3196	-0.5548	-1.0668	-0.2494
	SD				0.3658	-1.3599	-1.2452	-0.5367

Table 8 Comparison of the fundamental frequency  $\omega_1$  (Hz) from curved pipe regression formulas with previous results. All previous values were found using the FEM, except for case 7 (series solution using Donnel Mushtari theory)

Case	Ref.	Boundary condition and geometry					Fundamental frequency		
		Bdy.	$\psi_d$ (°)	$r$ (m)	$R/r$	$r/h$	Prev.	Regr.	% diff.
1	Red. 2004	CC	90	0.0858	2.66	12.1	2272	2499	10.0
2	Red. 2004	CC	90	0.1730	3.08	18.2	968	975	0.7
3	Red. 2004	CC	90	0.2492	3.06	26.1	664	632	-4.9
4	W,X&R '06	CC	90	0.0561	2.72	26.6	3152	3048	-3.3
5	W,X&R '06	SD	90	1.0	2.55	100	27	25	-9.2
6	W,X&R '06	SD	90	0.1	10	33.3	67	83	23.2
7	Red. 1994	SD	22.9	0.1	5.0	50.0	1153	1304	13.1

the SD condition there is strong dependence. As well, for the CC boundary condition there is relatively low dependence on the thickness ratio, while there is at least a moderate dependence for the SD condition. For both boundary conditions there is strong dependence on the radius ratio. There are again small but significant differences in the regression parameters for the two specified ranges of geometric parameters.

A comparison of frequencies obtained from the regression formulas with previous values is given in Table 8 for curved pipes. Cases 1-4 represent curved pipes having CC boundary conditions, while cases 5-7 are curved pipes with SD conditions. With a radius ratio of 12.1, case 1 is slightly outside of both specified geometric parameter ranges, and there is a sizeable difference between the previous and regression frequency values. Case 6 is at the extreme end of the radius ratio range (value of 10), and there is a large percentage difference between the previous and regression frequency values. A further look at results relevant to this parameter indicated that a limit in the range of  $R/r$  to 8 in the use of the regression formulas is in order. Generally, the agreement between the previous frequency values and the regression values is not as good as for the oblique cylindrical shell case, and the deviations in frequency for cases entirely within the range of geometric parameters may occasionally exceed 10%.

## 9. Conclusions

The trends in the natural frequencies of multiple 90° mitred pipe bends have been found using the finite element method based on shear-deformation shell elements. The results determined in the

parametric study indicate, as expected, that a relaxation of the boundary conditions or a decrease in the wall thickness leads to a significant decrease in the fundamental frequency. An increase in the cross-sectional radius or in the length of the tangent pipe leads to a modest decrease in the fundamental frequency. There are close similarities in the fundamental frequencies and vibration modes for the 2M, 3M, and C configurations. The 1M configuration on the other hand has some vibration characteristics that more closely resemble those of a straight pipe. Regression formulas for fundamental frequencies of cylindrical shells with one or two oblique edges showed smooth exponential variation with obliquity angle, length ratio, and thickness ratio. Similarly, regression formulas for curved pipes showed smooth exponential variation with bend angle, radius ratio, and thickness ratio. The results given provide information about the vibration characteristics of pipe bends over a wide range of the geometric parameters.

## References

- ADINA, AUI 8.2 (2003), *User Interface Primer and AUI Command Reference Manual*, ADINA R & D Inc., Watertown, MA.
- ANSYS (2005), *Release 10.0 - Documentation for ANSYS*, ANSYS Inc., Canonsburg, PA.
- Baylac, G. and Copin, A. (1975), "Vibration studies of the primary circuit of the Chinon 3 reactor", *Proceedings 3rd Int. Conf. on Struct. Mech. in React. Tech.*, Paper F4/3, London, Sept.
- Bert, C.W. and Malik, M. (1996), "Free vibration analysis of thin cylindrical shells by the differential quadrature method", *J. Pres. Ves. Tech.*, **118**, 1-12.
- Blevins, R.D. (1979), *Formulas for Natural Frequency and Mode Shape*, Van Nostrand Reinhold, New York.
- Budiansky, B. (1968), "Notes on nonlinear shell theory", *J. Appl. Mech.*, **35**, 393-401.
- Carneiro, J.O., de Melo, F.J.Q., Rodrigues, J.F.D., Lopes, H. and Teixeira, V. (2005), "The modal analysis of a pipe elbow with realistic boundary conditions", *Int. J. Pres. Ves. Pip.*, **82**, 593-601.
- Chang, D. and Redekop, D. (2007), "Collapse analysis of multiple 90° mitred pipe bends", *Proceedings 3rd Int. Conf. on Struct. Eng. Mech. & Comp. (SEMC 2007)*, Cape Town, Sept. 10-12, 8 pages.
- Chang, D. and Redekop, D. (2008), "Stress analysis of pressurized multiple 90° mitred pipe bends", *Proceedings 4th Int. Conf. on Advances in Struct. Eng. and Mech. (ASEM '08)*, Korea, 11 pages.
- Grimes, R.G., Lewis, J.G. and Simon, H.D. (1994), "A shifted block Lanczos algorithm for solving sparse symmetric generalized eigenproblems", *SIAM J. Matrix Anal. A.*, **15**(1), 228-272.
- Hinton, E., Sienz, J. and Özakça, M. (2003), *Analysis and Optimization of Prismatic and Axisymmetric Shell Structures*, Springer, Berlin.
- Hu, X.J. and Redekop, D. (2003), "Blending functions for vibration analysis of a cylindrical shell with an oblique end", *Int. J. Struct. Stab. Dyn.*, **3**, 405-418.
- Ming, R.S., Pan, J. and Norton, M.P. (2002), "Free vibrations of elastic circular toroidal shells", *Appl. Acoust.*, **63**, 513-528.
- Leissa, A.W. (1973), *Vibration of Shells*, NASA SP-288, Scientific and Technical Information Office, Washington.
- Orynyak, I.V., Radchenko, S.A. and Batura, A.S. (2007), "Calculation of natural and forced vibrations of a piping system. Part 2. Dynamic stiffness of a pipe bend", *Strength Mater.*, **39**(2), 144-158.
- Redekop, D. (1994), "Natural frequency of a short curved pipe", *Trans. CSME*, **18**, 35-45.
- Redekop, D. and Chang, D. (2008), "Linear vibration analysis of multiple 90° mitred pipe bends", *Proc. 3rd Int. Conf. on Advances in Struct. Eng. and Mech. (ASEM '08)*, Korea, 10 pages.
- Redekop, D. (2004), "Vibration analysis of a torus-cylinder shell assembly", *J. Sound Vib.*, **277**, 919-930.
- Salley, L. and Pan, J. (2002), "A study of the modal characteristics of curved pipes", *Appl. Acoust.*, **63**, 189-202.
- Soedel, W. (2006), *Vibration of Shells and Plates*, 3rd Ed., Marcell Dekker, New York.
- Shu, C. (2000), *Differential Quadrature and Its Application in Engineering*, Springer, Berlin.
- Wachel, J.C., Morton, S.H. and Atkins, K.E. (1990), "Piping vibration analysis", *Proc. 19th Turbomachinery*

- Symposium, College Station, Texas, 119-134.
- Wang, X.H., Xu, B. and Redekop, D. (2006), "Theoretical natural frequencies and mode shapes for thin and thick curved pipes and toroidal shells", *J. Sound Vib.*, **292**, 424-434.
- Wood, J. (2008), "A review of literature for the structural assessment of mitred bends", *Int. J. Pres. Ves. Pip.*, **85**(5), 275-294.